Bioorganic Chemistry 87 (2019) 736–742

Contents lists available at ScienceDirect

Bioorganic Chemistry

journal homepage: www.elsevier.com/locate/bioorg

Natural flavonoid α-glucosidase inhibitors from *Retama raetam*: Enzyme inhibition and molecular docking reveal important interactions with the enzyme active site

Usman Ghani[a,*], Mohammad Nur-e-Alam[b], Muhammad Yousaf[b], Zaheer Ul-Haq[c], Omar M. Noman[b], Adnan J. Al-Rehaily[b]

[a] Clinical Biochemistry Unit, Department of Pathology, College of Medicine, King Saud University, Riyadh 11461, Saudi Arabia
[b] Department of Pharmacognosy, College of Pharmacy, King Saud University, P.O. Box. 2457, Riyadh 11451, Saudi Arabia
[c] Dr. Panjwani Center for Molecular Medicine and Drug Research, International Center for Chemical and Biological Sciences, University of Karachi, Karachi 75210, Pakistan

ARTICLE INFO

Keywords:
Retama raetam
α-Glucosidase inhibitor
Flavonoid
Retamasin
Noncompetitive
Competitive
Molecular docking

ABSTRACT

Retama raetam (Forsk.) Webb & Berthel plant has been traditionally used for the treatment of diabetes mellitus and hypertension. Interest in the medicinal chemistry of the plant in the past resulted in the isolation of a number of compounds with anti-hyperglycemic activity. The current work is a further extension of our recent work in which we isolated and characterized seven new flavonoids from *Retama raetam* with preliminary biological activity screening. It addresses the α-glucosidase inhibitory activity and molecular docking studies of the flavonoids. Retamasin D, G, H, and erysubin A and B noncompetitively inhibited the enzyme whereas retamasin C and F exhibited competitive inhibition. Moreover, retamasin C, F, G, and erysubin A and B carry dual activity in addition to α-glucosidase inhibition. Our previous studies have shown that they also caused significant stimulation of insulin from the blood-perfused pancreatic islets of Langerhans of mice. The C6 and C8 substituent groups greatly influenced the inhibition potency of the compounds. The most potent inhibitor was retamasin H with the γ-lactone ring substituent at C6 position of the main flavonoid moiety. Notable active chemical groups in the target compounds include γ-lactone, dihydropyran and dihydrofuran rings with hydroxyl and geminal methyl groups. Molecular modeling studies revealed that the compounds fit well in the α-glucosidase active site by interacting with important active site residues. These findings will incorporate new chemical, structural and functional diversity to the search and drug development of α-glucosidase inhibitors as anti-diabetic drugs.

1. Introduction

Retama raetam (Forsk.) Webb & Berthel belongs to the Fabaceae family of plants that commonly grows in the Middle East, North Africa and Eastern Mediterranean region [1,2]. The plant is a halophyte and is abundant in the North-West region of Saudi Arabia as forage for cattles [3–5]. Traditionally, it has been used for the treatment of diabetes and hypertension in Saudi Arabia and Morocco [6]. Previous studies have confirmed that it lowers plasma glucose and lipid levels in normal and diabetic rats with concomitant anti-hypertensive activity [6–8]. Its hypoglycemic activity is proposed to be due to inhibition of glucose uptake by renal tubules [9]. Moreover, the biological activity profile of the plant also includes anti-microbial, anti-oxidant and insecticidal activities [10,11].

Interest in the medicinal chemistry of the plant with a special focus on potential anti-diabetic compounds is strongly supported by the evidence from the traditional medicinal use of the plant for diabetes treatment and from previous studies that identified some anti-hyperglycemic compounds from it. In this regard, a number of alkaloids including retamine, sparteine, lupinine and pinitol have been isolated form the plant. Pinitol has been shown to exhibit hypoglycemic activity. The folklore medicinal use of *Retama raetam* for diabetes treatment is scientifically supported by previous studies that have identified anti-hyperglycemic compounds from the plant [12–15], complemented by the current work, thus providing a detailed insight into the medicinal chemistry of the plant.

α-Glucosidases are important for carbohydrate digestion and processing that eventually maintain postprandial blood glucose levels. One

* Corresponding author.
E-mail addresses: ughani@ksu.edu.sa, ughani@gmx.net (U. Ghani), mohnalam@ksu.edu.sa (M. Nur-e-Alam).

https://doi.org/10.1016/j.bioorg.2019.03.079
Received 22 January 2019; Received in revised form 4 March 2019; Accepted 30 March 2019
Available online 01 April 2019
0045-2068/

way of controlling hyperglycemia in type 2 diabetes mellitus is to inhibit the enzyme to slow down intestinal carbohydrate digestion [16]. Clinically, there are only three oral α-glucosidase inhibitors (acarbose, miglitol and voglibose) currently prescribed for diabetes treatment beside other anti-diabetic drugs [17]. However, these drugs impose efficacy and side effect problems warranting further exploration and introduction of new potential anti-diabetic α-glucosidase inhibitors.

Significant interest in the identification of flavonoid constituents of *Retama raetam* has led to discovery of luteolin 4′-neohespiridoside, atalantoflavone, saponarin, retamasin A and B, licoflavone C, genistein 8-C-glucoside and ephedroidin [18,19]. Flavonoids are polyphenolic secondary metabolites widely present in plants, fruits and vegetables. They are regarded as an important class of compounds in a number of pharmaceutical, medicinal and nutraceutical products because of their therapeutic effects. Flavonoids are abundant in nature with a spectrum of biological activities including anti-inflammatory, anti-carcinogenic, and anti-oxidative activities. A variety of flavonoids have been identified as promising α-glucosidase inhibitors that include kaempferol, quercetin, kaempferol 3-*O*-β-glucopyranoside, quercetin 3-*O*-(3″-*O*-galloyl)-β-galactopyranoside, quercetin 3-*O*-(6″-*O*-galloyl)-β-glucopyranoside [20], acylated flavonol rhamnosides, broussochalcone A, dorsilurin F and G [21].

We recently isolated and characterized seven new flavonoids from *Retama raetam* that included three flavones namely retamasin C–E and four isoflavones retamasin F–I. Retamasin C, E, F, G and erysubin A and B showed significant stimulation of insulin from the blood-perfused pancreatic islets of Langerhans of mice. All compounds except erysubin A exhibited more insulin secretion activity than the standard insulin secretagogue tolbutamide [22]. The current work is a further extension of our recent work that involves our continuing efforts to identify potential α-glucosidase inhibitors that may become candidates for anti-diabetic drug development. We report α-glucosidase inhibitory activity, enzyme kinetic studies of the flavonoids namely retamasin C, D, F, G, H, and erysubin A and B. Furthermore, retamasin C and F were also subjected to molecular docking studies that has revealed important information on active site binding of the compounds. Retmasin D, G, H, and erysubin A and B noncompetitively whereas retamasin C and F competitively inhibited α-glucosidase enzyme. Retamasin C, F, G, and erysubin A and B carry dual activities; they stimulate insulin secretion and also inhibit α-glucosidase enzyme. The dual action gives the compounds a special advantage over others in terms of becoming promising candidates for anti-diabetic drug development. Therefore, the current work will incorporate new structural and functional diversity to drug discovery of anti-diabetic drugs.

2. Materials and methods

2.1. Extraction, isolation and structure elucidation of the compounds

The extraction and isolation of the compounds from the aerial parts of *Retama raetam* along with structure elucidation has been reported in our recent publication [22].

2.2. α-Glucosidase inhibition assay

The α-glucosidase inhibition assay was adapted from the previously reported method [23] which was modified for the current work. A 96-well microplate format was used for all assays. The total volume of the reaction mixture was 300 µl that contained sodium phosphate buffer (50 mM; pH 6.8), 40 mU of α-glucosidase from *Saccharomyces cerevisiae* (Sigma Chemical Co., St. Louis, USA) and the substrate *p*-nitrophenyl-α-D-glucopyranoside (0.7 mM). The compounds of interest were dissolved in DMSO and the final concentration of DMSO in the reaction mixture was 3%. The enzyme was first incubated with the compounds at 37 °C for 15 min. followed by addition of the substrate to initiate the enzyme reaction. The reaction was constantly monitored in 96-well microplates using SpectraMax Plus 384® microplate reader at 400 nm. (Molecular Devices, CA, USA). Negative control experiments containing no compounds were also run in parallel. Acarbose was used as a positive control. Each assay was conducted in four separate experiments and the mean values were calculated with SEM (standard error of mean).

2.3. α-Glucosidase inhibition kinetics

The assay protocol adapted for kinetic studies was the same as above except that it was modified as per experimental requirements. The assay mixture contained various concentrations of the target compounds and a range of substrate concentrations (*p*-nitrophenyl-α-D-glucopyranoside 0.25–2.0 mM). The initial velocities of the enzyme were determined in the presence and absence of the compounds using only the linear portion of the enzyme velocity curves. The Lineweaver-Burk plots were constructed to determine the type of inhibition, and the K_i values of the inhibitors were calculated by the Dixon plot using Grafit 7.0.3 (Erithacus Software Ltd., Staines, UK). Each kinetic assay was performed in quadruplicate from which mean K_i values and the SEM were calculated.

2.4. Computational studies

The molecular docking simulation studies were performed using Swiss Modeller. The homology modeling was performed using the protocol reported elsewhere [24]. The homology model of yeast α-glucosidase was based on the crystal structure of isomaltase from *Saccharomyces Cerevisiae* as a template. The compounds were built using the builder module in MOE 2018.0101 (Molecular Operating Environment 2013.08; Chemical Computing Group ULC, Montreal, Canada) with subsequent application of charges and minimization using MMFF94x forcefield [25].

The molecular docking simulation was carried out using MOE-dock with default docking protocols. For each compound 30 poses were generated. The active site was identified using the coordinates of cognate maltose from the Protein Data Bank (PDB identifier: 3A4A) [26]. The top-ranked pose of each ligand was analyzed visually. The images were rendered using PLIP web server [27].

3. Results and discussion

3.1. α-glucosidase inhibition and kinetic studies

The compounds significantly decreased the α-glucosidase rate of reaction in a concentration-dependent manner when compared to the negative controls that contained no inhibitors. The compounds displayed a variable degree of inhibitory activities as indicated by their K_i values. Some compounds exhibited comparable K_i values while others had marked activity differences between them. The structures and K_i values of the compounds are listed in Table 1. The K_i values of the compounds ranged from 12.06 to 71.17 µM. Since the compounds possess a variety of substituent chemical groups beside similar flavonoid parent structure, it is obvious to explain that the differences in their inhibition potency are mainly because of the substituent groups. In this regard, an account on the identification of active chemical groups along with a comparative discussion on their inhibition potencies will follow.

The observed inhibition kinetic data was first analyzed using the Michaelis-Menten equation, which was screened for best fit into the Lineweaver-Burk plot [28] for determining the type of inhibition. Data, only with least standard of error, were considered for best-fit analysis. Retamasin C and F exhibited competitive inhibition of the enzyme as indicated by their corresponding Lineweaver-Burk plots showing variable *x*-intercepts with all lines converging at the same point on the *y*-axis typical of competitive inhibition. The apparent K_m ($K_{m,app}$) value was calculated from each *x*-axis intercept at each [I]. Dixon plots were

Table 1
The structures of the flavonoids with their K_i values and the type of inhibition. Each K_i value represents the mean value of four separate experiments with SEM.

Compound name and type	Structure	K_i (μM ± SEM)	Type of inhibition
Retamasin C (Flavone)	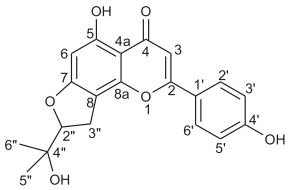	19.93 ± 0.77	Competitive
Retamasin D (Flavone)	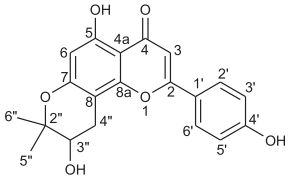	39.17 ± 0.86	Noncompetitive
Retamasin F (Isoflavone)	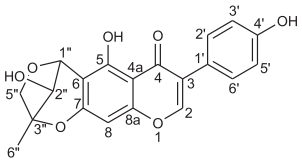	14.45 ± 0.83	Competitive
Retamasin G (Isoflavone)	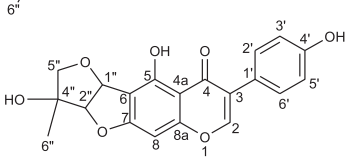	56.61 ± 0.95	Noncompetitive
Retamasin H (Isoflavone)	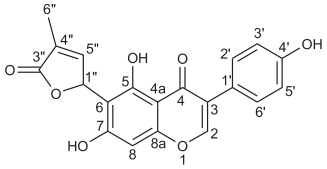	12.06 ± 0.57	Noncompetitive
Erysubin A (Isoflavone)	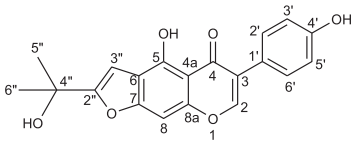	16.42 ± 0.18	Noncompetitive
Erysubin B (Isoflavone)	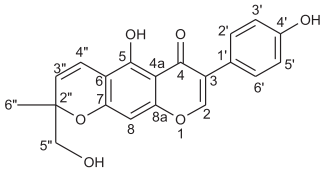	71.17 ± 0.64	Noncompetitive
Acarbose		4.72 ± 0.38	Competitive

constructed and the K_i values were directly calculated from the *y*-axis intercept of the plots, the pattern of which also complied with competitive inhibition [29]. The V_{max} and K_m values were in agreement with competitive inhibition that is characterized by an increase in K_m with no change in V_{max} value (Fig. 1A).

The Lineweaver-Burk plots for retamasin D, G, H, and erysubin A and B showed noncompetitive inhibition of α-glucosidase. The plots displayed variable *y*-intercepts with all lines converging at the same point on the *x*-axis, conforming to noncompetitive inhibition. From each *y*-axis intercept, the apparent V_{max} ($V_{max,app}$) value was calculated at each [I]. The K_i values were calculated directly from the *x*-axis intercept of the Dixon plots {$1/v$ versus [I]}, which also agreed with noncompetitive inhibition [29]. The V_{max} and K_m values were in conformity to noncompetitive inhibition that is characterized by a decrease in V_{max} and no change in K_m value (Fig. 1B).

The Lineweaver-Burk and their corresponding Dixon plots for representative noncompetitive and competitive inhibitors are presented in Fig. 2 and Fig. 3, respectively.

3.2. Identification of active chemical groups

All of the isoflavones and flavones studied in the current work carried C6 and C8 substitutions respectively. Interestingly in all of these substitutions, the hydroxyl and methyl groups terminally flank as side groups, which are either in single or in germinal configuration. As mentioned earlier, the variability in inhibition potencies of the target compounds is mainly influenced by these substitutions along with the hydroxyl and methyl groups beside the parent flavonoid moiety. The most potent inhibitor in the series was retamasin H (K_i = 12.06 μM), an isoflavone possessing a γ-lactone substituent at C6 of the main moiety that noncompetitively inhibited α-glucosidase. The potent activity of the compound appears to be mainly due to presence of the γ-lactone

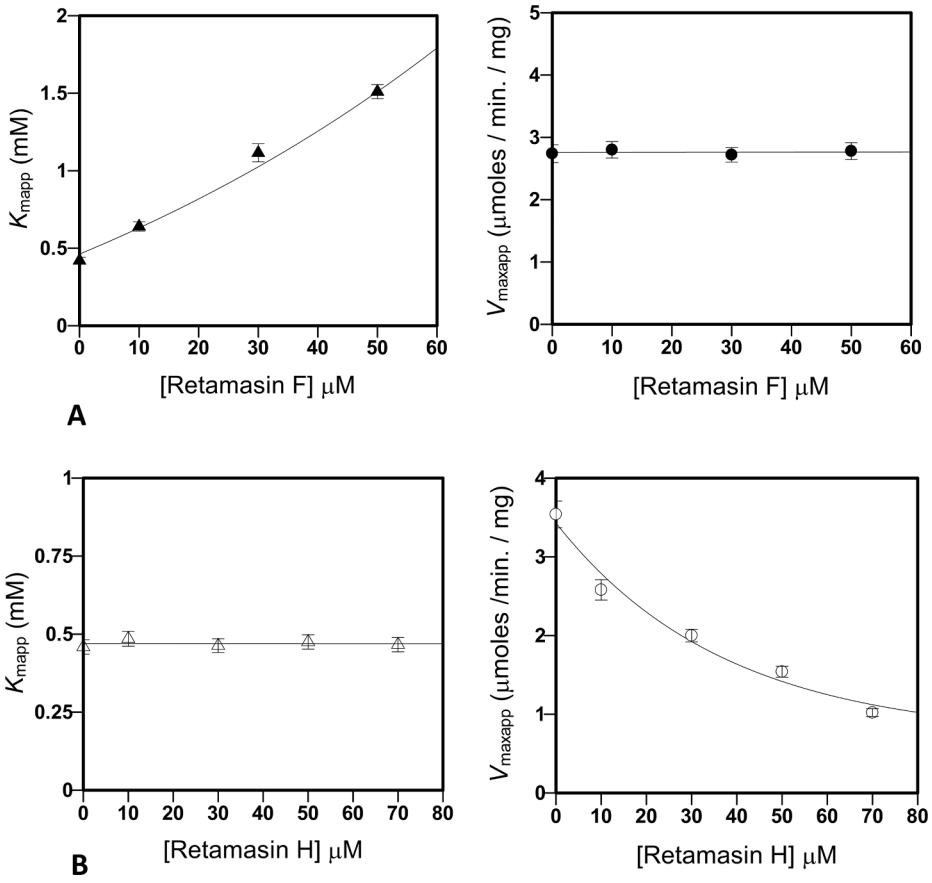

Fig. 1. (A). Representative graphs for the competitive inhibitors indicating increasing K_{mapp} with no change in the V_{maxapp} value consistent with the competitive inhibition of the enzyme. **(B)**. Representative graphs for the noncompetitive inhibitors indicating decreasing V_{maxapp} with no change in the K_{mapp} value consistent with the noncompetitive inhibition of the enzyme.

side chain.

The inhibitory activities of retamasin D (carrying a dihydropyran ring at C8 of the main flavone moiety with geminal methyl groups), and retamasin C (carrying a dihydrofuran ring with germinal methyl groups) bear a marked difference despite both carrying germinal methyl groups. The only contrasting structural difference between these two inhibitors is due to the dihydropyran and a dihydrofuran rings. Since both of the compounds are structural isomers and not stereoisomers, comparison between them will provide little information in terms of structure and activity relationship. Since they are different only because of the dihydropyran and dihydrofuran rings, a limited comparison is still possible that may conclude to some extent that the dihydrofuran ring with germinal methyl groups in retamasin C is more important for potent inhibition of α-glucosidase.

Erysubin B, bearing a dihydropyran ring with the methyl and hydroxyl groups at C6 of the isoflavone moiety, inhibited the enzyme with a K_i value of 71.17 μM. Its potency improved more than 4-fold when its C6 substitution is replaced by a lactone ring carrying a hydroxyl group and geminal methyl groups, as seen in erysubin A (K_i = 16.42 μM). It is noteworthy to mention that retamasin H, the most potent compound in the series, also possessed a lactone ring and a methyl group at the same position. Therefore, it is apparent that the presence of the lactone ring bound to a hydroxyl and geminal methyl groups at C6 position of the isoflavone moiety contributes to potent inhibition of α-glucosidase.

Interestingly, the type of C6 substitution in retamasin F is unique among all the compounds studied in the current work; it possesses a bicycle fused to the isoflavone core at C6 and C7 positions with a C2″ methine (K_i = 14.45 μM). In fact, it is found to be next most potent competitive inhibitor after retamasin H with the K_i value comparable to that of erysubin A and retamasin C.

From these studies, a number of active groups have been identified in the target compounds that contributed to potent α-glucosidase inhibition. These include γ-lactone, fused bicycle moiety with C2″ methine, and dihydrofuran ring with a hydroxyl and geminal methyl groups.

3.3. Molecular modeling studies

Retamasin C (K_i = 19.93 μM) and F (K_i = 14.45 μM) were subjected to molecular modeling studies as representative compounds from the flavones and isoflavones, respectively. These studies were aimed at determining how the target compounds apparently bind to the α-glucosidase active site.

A homology model of the yeast α-glucosidase was developed using the crystal structure of isomaltase from *Saccharomyces cerevisae* as a template. The docking score analysis revealed that both of the target compounds were well accommodated in the active site with the docking scores of −5.68 and −5.80 for retamasin C and F, respectively. Fig. 4A displays the modeled retamasin C-active site complex. It is evident that the inhibitor forms a number of polar and nonpolar interactions with the active site residues of the enzyme. The hydroxyl group, beside the geminal methyl groups and in proximity to the dihydrofuran ring, mediates hydrogen bonding with Asp349 and Arg439, which are the important catalytic residues of the enzyme. The hydrogen atom of the hydroxyl group on the 4″-position of the benzene ring is involved in polar contact with Asn347. The π-stacking interactions between Phe298, Phe300 and the inhibitor further stabilize the contacts (Table 2).

Fig. 4B presents the modeled retamasin F-active site complex. It is evident that the inhibitor mediates hydrophobic contacts with the residues of the active site hydrophobic patch that includes Phe157, Phe177 and Phe300. Moreover, the hydroxyl group on the C2″ methine is involved in the hydrogen bonding interaction with Asp68, Arg312 and Arg439 residues (Table 2). As mentioned earlier, the C2″ methine in retamasin F is part of the bicycle fused to the isoflavone core at C6 and C7 positions.

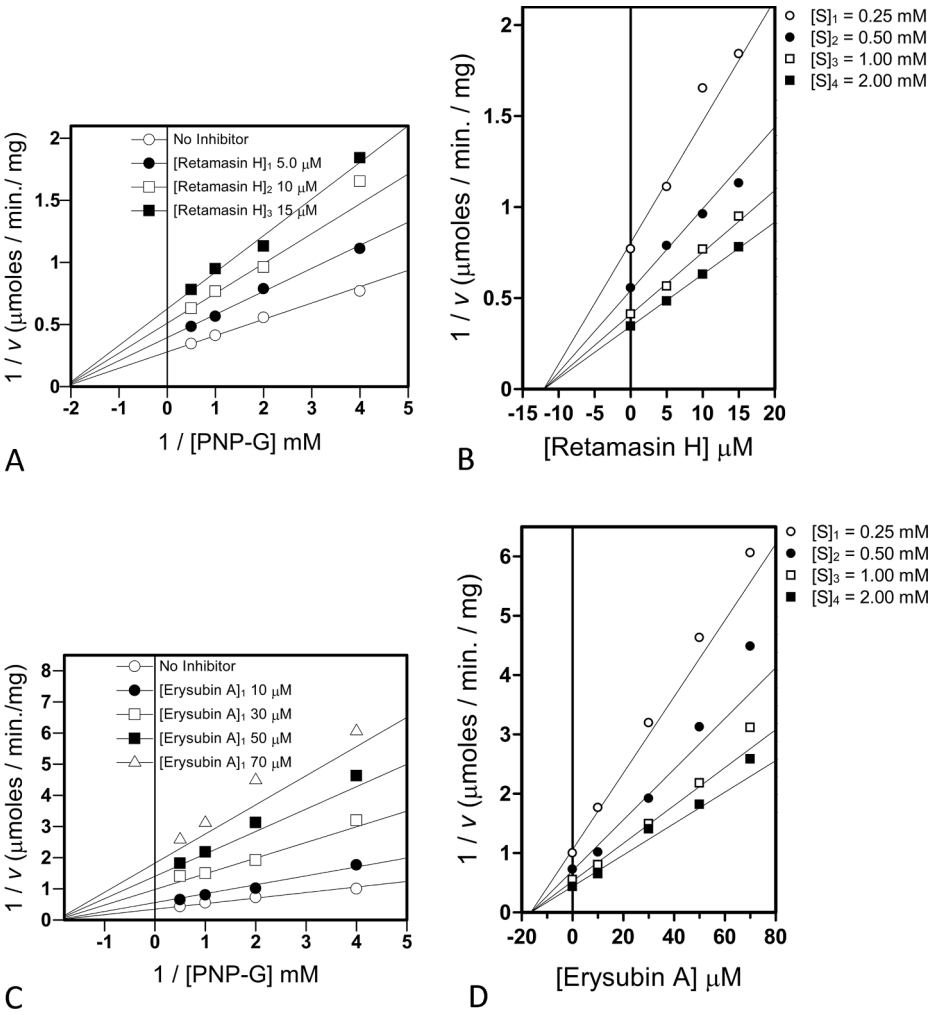

Fig. 2. Representative Lineweaver-Burk (A, C) and Dixon plots (B, D) for the noncompetitive inhibitors.

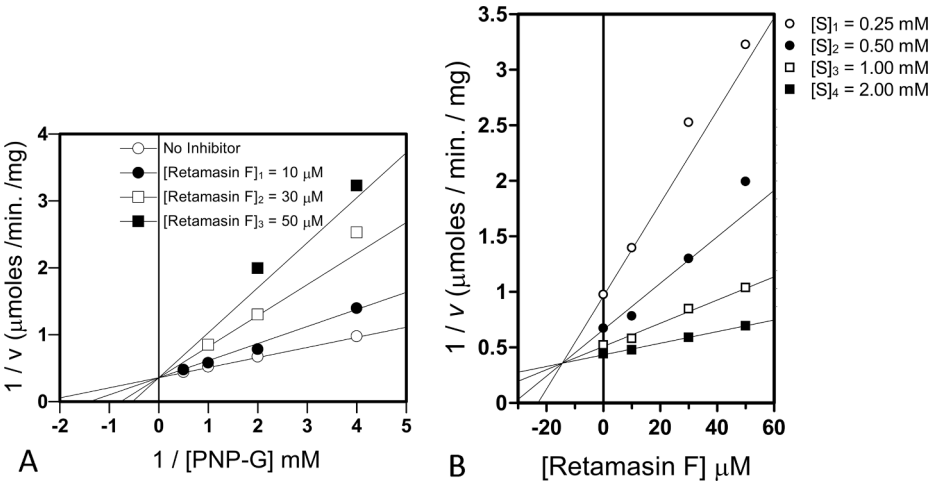

Fig. 3. Representative Lineweaver-Burk (A, C) and Dixon plots (B, D) for the competitive inhibitors.

4. Conclusions

Retama raetam is used for the treatment of diabetes mellitus and hypertension in traditional medicine. Previous studies have complemented the therapeutic properties of the plant by isolating a number of compounds with anti-hyperglycemic activity. Our work has identified seven flavonoids with α-glucosidase inhibitory activity, majority of which were noncompetitive inhibitors. Generally, the inhibitory potency of majority of the target compounds was comparable to each other. The C6 substitutions in isoflavones and C8 substitutions in flavones greatly influenced the α-glucosidase inhibitory activity. These substitutions include γ-lactone, fused bicycle moiety with C2″ methine, hydroxyl and geminal methyl groups. Additionally, retamasin C, F, G, and Erysubin A and B showed promising dual activity by stimulating

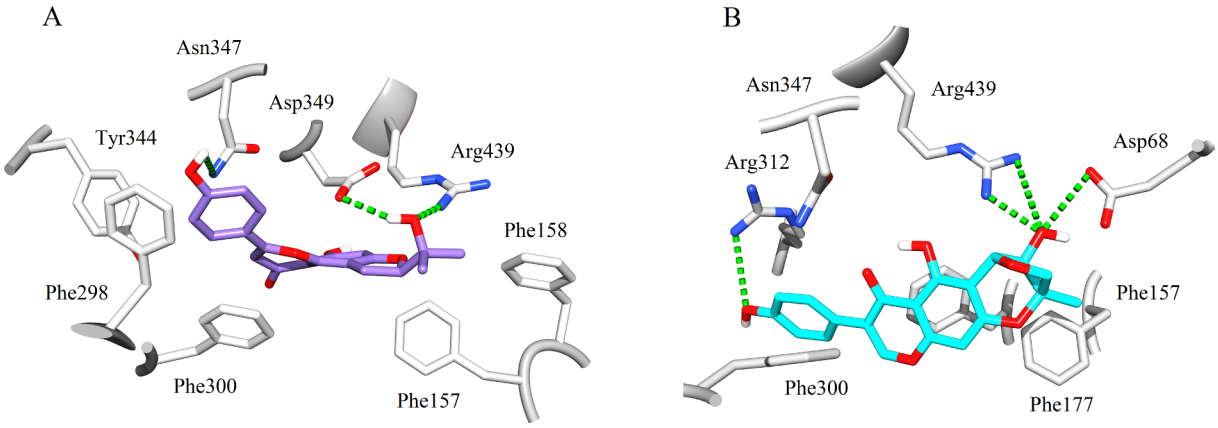

Fig. 4. The simulated binding pose of (**A**) retamasin C and (**B**) retamasin F. The α-glucosidase active site residues are presented as sticks, the carbon atoms are colored in grey, the oxygen atoms in red and the nitrogen atoms in blue. The carbon atoms of retamasin C and F are depicted in two different colors. The hydrogen bonds are represented as green dashes. The image was rendered using Chimera [30] and Ray-trace using POVRAY [31].

Table 2
The protein-ligand interaction profiles of (**A**) retamasin C and (**B**) retamasin F in complex with α-glucosidase obtained from the PLIP web server.

Residue #	Amino acid	Distance (Å)
A		
Hydrophobic interactions		
57A	TRP	3.83
157A	PHE	3.16
158A	PHE	3.44
298A	PHE	3.30
300A	PHE	3.03
344A	TYR	3.46
Hydrogen bonds		
312A	ARG	3.48
347A	ASN	2.75
349A	ASP	2.44
300A	PHE	3.60
B		
Hydrophobic interactions		
157A	PHE	2.99
157A	PHE	3.20
177A	PHE	3.50
177A	PHE	3.23
300A	PHE	3.11
Hydrogen bonds		
68A	ASP	1.73
312A	ARG	2.61
439A	ARG	1.78
439A	ARG	3.02
π Stacking		
300A	PHE	4.71

insulin secretion from the mice pancreatic islets of Langerhans and inhibiting α-glucosidase enzyme. These compounds may especially become potential candidates for anti-diabetic drug development especially due to their dual activities. Molecular modeling studies on retamasin C and F showed that the compounds accommodate well in the active site pocket of α-glucosidase by interacting with a number of important residues of the active site. The inhibitors and their apparent interactions with the α-glucosidase active site along with the active chemical groups identified in the current work will open new avenues to the drug development of promising anti-diabetic drugs.

Conflict of interest

The authors declare no conflict of interest.

Acknowledgement

The authors would like to thank the Deanship of Scientific Research at King Saud University for funding the research group through project number RGP-1438-043.

References

[1] R. Mittler, E. Merquiol, E. Hallak-Herr, Living under a “dormant” canopy: a molecular acclimation mechanism of the desert plant Retama raetam, Plant J. 25 (2001) 407–416.
[2] L. El Bahri, M. Djegham, H. Bellil, *Retama raetam* W: a poisonous plant of North Africa, Vet. Human Toxicol. 41 (1999) 33–35.
[3] V. Laudadio, V. Tufarelli, M. Dario, M. Hammadi, M.M. Seddik, G.M. Lacalandra, C. Dario, A survey of chemical and nutritional characteristics of halophytes plants used by camels in Southern Tunisia, Trop. Animal Health Prod. 41 (2009) 209–215.
[4] S. Boufennara, S. Lopez, H. Bousseboua, R. Bodas, L. Bouazza, Chemical composition and digestibility of some browse plant species collected from Algerian arid rangelands, Spanish J. Agric. Res. 10 (2012) 88–98.
[5] N.A.M. Barakat, V. Laudadio, E. Cazzato, V. Tufarelli, Potential contribution of *Retama raetam* (Forssk.) Webb & Berthel as a Forage Shrub in Sinai, Egypt, Arid Land Res. Manage. 27 (2013) 257–271.
[6] M. Maghrani, A. Lemhadri, H. Jouad, J.-B. Michel, M. Eddouks, Effect of the desert plant Retama raetam on glycaemia in normal and streptozotocin-induced diabetic rats, J. Ethnopharmacol. 87 (2003) 21–25.
[7] M. Maghrani, A. Lemhadri, N.-A. Zeggwagh, A. El Amraoui, M. Haloui, H. Jouad, M. Eddouks, Effect of *Retama raetam* on lipid metabolism in normal and recent-onset diabetic rats, J. Ethnopharmacol. 90 (2004) 323–329.
[8] M. Maghrani, N.-A. Zeggwagh, M. Haloui, M. Eddouks, Acute diuretic effect of aqueous extract of *Retama raetam* in normal rats, J. Ethnopharmacol. 99 (2005) 31–35.
[9] M. Maghrani, J.B. Michel, M. Eddouks, Hypoglycaemic activity of *Retama raetam* in rats, Phytother. Res. 19 (2005) 125–128.
[10] S. Mariem, F. Hanen, J. Inès, S. Mejdi, K. Riadh, Phenolic profile, biological activities and fraction analysis of the medicinal halophyte *Retama raetam*, S. African J. Botany 94 (2014) 114–121.
[11] E. Hayet, M. Maha, A. Samia, M. Mata, P. Gros, H. Raida, M.M. Ali, A.S. Mohamed, L. Gutmann, Z. Mighri, A. Mahjoub, Antimicrobial, antioxidant, and antiviral activities of *Retama raetam* (Forssk.) Webb flowers growing in Tunisia, World J. Microbiol. Biotechnol. 24 (2008) 2933–2940.
[12] A. El Shazly, A.M. Ateya, L. Witte, M.Z. Wink, Quinolizidine alkaloid Profiles of *Retama raetam*, R. sphaerocarpa and R. monosperma, Naturforschung C 51 (1996) 301–308.
[13] G. Faugeras, M.H. Meyruey, R. Paris, On the alkaloids of *Retama raetam* Webb and Berth. (Genista raetam Forsk.). II. Isolation of anagyrine from flowers, Pharm. Françaises 21 (1963) 675–679.
[14] G. Faugeras, M.H. Meyruey, R. Paris, On the alkaloids of Retama raetam Webb and Berth. (Genista raetam Forsk.). Isolation of cytisine from the fruit, Ann. Pharm. Françaises 20 (1962) 768–776.
[15] N.H. González-Mauraza, A.J. León-González, J.L. Espartero, J.B. Gallego-Fernández, M. Sánchez-Hildago, C. Martin-Cordero, Isolation and quantification of pinitol, a bioactive cyclitol Retama spp. Nat. Prod. Commun. 11 (2016) 405–406.
[16] K.C. Maki, M.L. Carson, M.P. Miller, M. Turowski, M. Bell, D.M. Wilder, M.S. Reeves, High-viscosity hydroxypropylmethylcellulose blunts postprandial glucose and insulin responses, Diabetes Care 30 (2007) 1039–1043.
[17] A.J. Krentz, C.J. Bailey, Oral antidiabetic agents: current role in type 2 diabetes mellitus, Drugs 65 (2005) 385–411.
[18] M. Kassem, S.A. Mosharrafa, N.A.M. Saleh, S.M. Abdel-Wahab, Two new flavonoids

from *Retama raetam*, Fitoterapia 71 (2000) 649–651.
[19] W.-H. Xu, A.J. Al-Rehaily, M. Yousaf, M.S. Ahmad, S.I. Khan, I.A. Khan, Two new flavonoids from *Retama raetam*, Helv. Chim. Acta 98 (2015) 561–568.
[20] A.N. Panche, A.D. Diwan, S.R. Chandra, Flavonoids: an overview, J. Nutr. Sci. 5 (2016) 1–15.
[21] U. Ghani, Re-exploring promising -glucosidase inhibitors for potential development into oral anti-diabetic drugs: finding needle in the haystack, Eur. J. Med. Chem. 103 (2015) 133–162.
[22] M. Nur-e-Alam, M. Yousaf, I. Parveen, M. Rahman, U. Ghani, S. Ahmed, A. Hameed, M. Threadgill, M. AL-Rehaily, New flavonoids from the Saudi Arabian plant *Retama raetam* which stimulates secretion of insulin and inhibits α-glucosidase, Org. Biomol. Chem. 17 (2019) 1266–1276.
[23] K. Ma, J. Han, L. Bao, T. Wei, H. Liu, Two sarcoviolins with antioxidative and α-glucosidase inhibitory activity from the edible mushroom *Sarcodon leucopus* collected in Tibet, J. Nat. Prod. 77 (2014) 942–947.
[24] A. Barakat, M. Ali, M.A. Al-Majid, S. Yousuf, M.I. Choudhary, R. Khalil, Z. Ul-Haq, Synthesis of thiobarbituric acid derivatives: in vitro α-glucosidase inhibition and molecular docking studies, Bioorg. Chem. 75 (2017) 99–105.
[25] T.A. Halgren, Merck molecular force field I. Basis form, scope, parameterization and performance of MMFF94, J Comput. Chem. 17 (1996) 490–519.
[26] K. Yamamoto, H. Miyake, M. Kusunoki, S. Osaki, Crystal structures of isomaltase from *Saccharomyces cerevisiae* and in complex with its competitive inhibitor maltose, FEBS J. 277 (2010) 4205–4214.
[27] S. Sebastian, S. Schreiber, V.J. Haupt, M.F. Adasme, M. Schroeder, PLIP: fully automated protein-ligand interaction profiler, Nucleic Acids Res. 43W1 (2015) W443–W447.
[28] H. Lineweaver, D. Burk, The determination of enzyme dissociation constants, J. Am. Chem. Soc. 56 (1934) 658–666.
[29] M. Dixon, The determination of enzyme inhibitor constants, Biochem. J. 55 (1953) 170–171.
[30] E.F. Pettersen, T.D. Goddard, C.C. Huang, G.S. Couch, D.M. Greenblatt, E.C. Meng, T.E. Ferrin, UCSF chimera–a visualization system for exploratory research and analysis, J. Comput. Chem. 25 (2004) 1605–1612.
[31] C.J. Cason, T. Froehlich, N. Kopp, R. Parker, POV-RAY, Persistence Vis. Raytracer Pty. Ltd., Victoria, Australia, 2003.